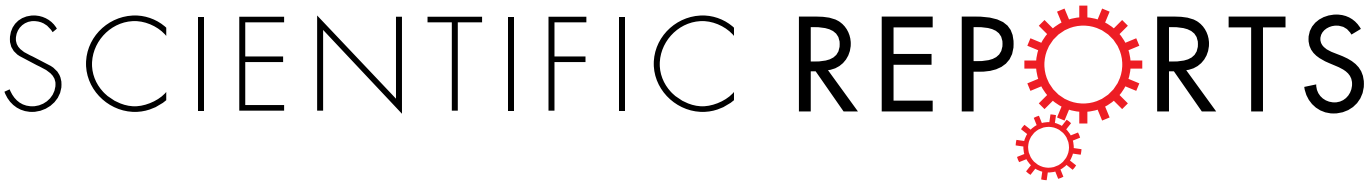

OPEN

Received: 19 April 2016
Accepted: 04 July 2016
Published: 02 August 2016

Experimental validation of non-uniformity effect of the radial electric field on the edge transport barrier formation in JT-60U H-mode plasmas

K. Kamiya[1], K. Itoh[2] & S.-I. Itoh[3,4]

The turbulent structure formation, where strongly-inhomogeneous turbulence and global electromagnetic fields are self-organized, is a fundamental mechanism that governs the evolution of high-temperature plasmas in the universe and laboratory (e.g., the generation of edge transport barrier (ETB) of the H-mode in the toroidal plasmas). The roles of inhomogeneities of radial electric field (E_r) are known inevitable. In this mechanism, whether the first derivative of E_r (shear) or the second derivative of E_r (curvature) works most is decisive in determining the class of nontrivial solutions (which describe the barrier structure). Here we report the experimental identification of the essential role of the E_r-curvature on the ETB formation, for the first time, based on the high-spatiotemporal resolution spectroscopic measurement. We found the decisive importance of E_r-curvature on ETB formation during ELM-free phase, but there is only a low correlation with the E_r-shear value at the peak of normalized ion temperature gradient. Furthermore, in the ELMing phase, the effect of curvature is also quantified in terms of the relationship between pedestal width and thickness of the layer of inhomogeneous E_r. This is the fundamental basis to understand the structure of transport barriers in fusion plasmas.

Since the discovery in ASDEX tokamak[1], the high confinement mode (H-mode) was studied on many tokamaks, leading to the "baseline" operation scenario for ITER[2]. Theoretical work predicted that the edge radial electric field, E_r, should play an important role in the mechanism of the L-H transition[3]. The key idea is the self-organized dynamics of strong radial electric field and suppression of transport[3–5], as is summarized in[6]. According to theoretical predictions, extensive measurements for the ion density, temperature, and poloidal/toroidal flows at the plasma peripheral region were performed by means of spectroscopic method[7,8], and experimental verifications on many devices were also performed[9–11], exhibiting the localized E_r and significant reduction in a plasma turbulence level. It is conventionally believed that the shear of $\boldsymbol{E}\times\boldsymbol{B}$ drift velocity (*i.e.* first derivative of E_r) is the main parameter that is responsible for suppression of turbulence[5,12–15]. In addition, the important role of the curvature of radial electric field (*i.e.* second derivative of E_r) in suppressing the turbulence and turbulent transport has also been pointed out[16–20]. However, there has been no quantitative verification for both E_r-shear and curvature effects on the ETB formation, simultaneously, due to lack of diagnostic that can withstand up to the second derivative estimation. Whether the first derivative or the second derivative works most in turbulence suppression is decisive in determining of class of nontrivial solutions (as has been theoretically pointed out[21]). The influence of the curvature of E_r has been more widely investigated when one considers the excitation of Zonal flows (ZFs) by the drift wave (DW) turbulence (see, a review[22]). The discrimination of roles of the shear and curvature of E_r in reducing turbulence is essential. This is because, these two represent the two fundamental processes in turbulent structure formation, i.e., (1) the enhanced dissipation of DW fluctuations and (2) the convergence of

[1]National Institutes for Quantum and Radiological Science and Technology (QST), Naka, Ibaraki-ken 311-0193, Japan. [2]National Institute for Fusion Science (NIFS), Toki, Gifu 509-5292, Japan. [3]Research Institute for Applied Mechanics, Kyushu University, Kasuga, Kasuga koen 6-1, 816-8580, Japan. [4]Research Center for Plasma Turbulence, Kyushu University, Kasuga 816-8580, Japan. Correspondence and requests for materials should be addressed to K.K. (email: kamiya.kensaku@qst.go.jp)

DW energy into coherent axial vector fields, respectively. It is also important for understanding the formation of transport barriers in toroidal confinement devices. For instance, the "curvature transition", a kind of the internal transport barriers[23], looks to appear in conjunction with the E_r curvature. The trapping of turbulence intensity in the trough of E_r [24] has also been observed[25,26]. Here we report the experimental identification of the essential role of inhomogeneities of E_r on the ETBs formation, for the first time, based on the high-spatiotemporal resolution spectroscopic measurement[27–29], being to develop the quantitative examination of two independent (i.e. E_r-shear and -curvature) effects on ETBs formation. It is shown that both the shear and curvature of E_r work, but the role of curvature is inevitable in the formation of transport barrier. This discovery has a fundamental impact on our understanding of structure formation in magnetized plasmas, in addition to a substantial impact on our predictability of performance of future burning plasma experiments, since the over-all performance of toroidal plasma fusion device critically depends on the property of the ETB. For instance, the uncertainty in the fusion power amplification factor of ITER was estimated as about factor 10, and the main origin for which is the variance in the prediction of the width of the ETB[30].

Results

Theoretical model. The model of turbulence intensity, in the presence of inhomogeneous radial electric field, was assessed based on the model formula for the effect of electric field shear[5,12,13] and that of electric field curvature in[31,32], and is used in the experimental test here as;

$$I = \{1 + (k\rho_i)^{-2}Z\}^{-1}I_0. \tag{1}$$

where the parameters are as follows:

$$Z = Z_1 + Z_2,$$

$$[Z_1 \equiv \{\rho_i^{\,2}(V_dB)^{-2}\}(E_r'E_r') \quad \text{and} \quad Z_2 \equiv \{\rho_i^{\,2}(V_dB)^{-2}\}(-E_r^*E_r'')] \tag{2}$$

I is the turbulence intensity (mean square of fluctuation velocity normalized to the diamagnetic speed), ρ_i is the ion gyro-radius, k is a typical wavenumber for the plasma turbulence, V_d is the diamagnetic velocity ($V_d \equiv \mathrm{T}/eaB$), e: elementary charge, a: characteristic mean-scalelength, B: total magnetic field), $E_r^* \equiv E_r - (V_\phi^{C6+} \times B_\theta)$ is the modified radial electric field subtracting the toroidal rotation component (estimated by the product of the toroidal rotation velocity for fully tripped carbon impurity ions, V_ϕ^{C6+}, and poloidal magnetic field, B_θ), and I_0 is the mean intensity in the limit of $Z = 0$. The term Z_1 and Z_2 denote the effects of E_r-shear (*i.e.* first derivative of E_r defined as $E_r' \equiv \frac{dE_r}{dr}$)[5,12,13] and E_r-curvature (*i.e.* second derivative of E_r defined as $E_r'' \equiv \frac{d^2E_r}{dr^2}$)[31], respectively. [Note that the correction for the effect of toroidal flow is necessary only for the E_r value in the Z_2 term. This is because the force by turbulent Reynolds stress ($\langle \widetilde{V}_r \widetilde{V}_\theta \rangle \propto \frac{dE_r}{dr}$) is mainly in the poloidal direction, and its work is the product of force and poloidal velocity (not $\boldsymbol{E} \times \boldsymbol{B}$ velocity) as $V_\theta \frac{d}{dr}\langle \widetilde{V}_r \widetilde{V}_\theta \rangle \propto E_r^* \frac{d^2E_r}{dr^2}$.] The term Z_2 has its sign dependence.

In association with the turbulence reduction by the inhomogeneous E_r, the temperature gradient is enhanced. If one employs the gyroBohm dependence of local thermal diffusivity, which is proportional to the temperature gradient and turbulent intensity, the heat flux is proportional to the turbulence intensity multiplied by $(\nabla T)^2$. For fixed heat flux, one can evaluate the enhancement degree of the ion temperature gradient in terms of Z value as;

$$\frac{L_{T_i}^{-1}(H - phase)}{L_{T_i}^{-1}(L - phase)} \approx (k\rho_i)^{-1}\sqrt{Z}. \tag{3}$$

Here, the $L_{T_i}^{-1}$ is the normalized ion temperature gradient ($L_{T_i}^{-1} \equiv -\nabla T_i/T_i$). The characteristic value of the wave number has been considered to be $k\rho_i \sim 0.1 - 0.3$ [33]. In the present examination, the wavelength of fluctuations is not measured, so that the proportionality between the ratio of gradient scale lengths and the parameters Z_1, Z_2, and Z are investigated. When the turbulent transport is reduced to the level of neoclassical transport, further reduction of turbulence level is less effective in increasing the ion temperature gradient.

Experimental results (I): Temporal dynamics in ELM-free phase. In examining the effect of non-uniformity of E_r on the ETBs formation, Fig. 1 (discharge E049219 with balanced-NBI heating) exhibits the illuminating data that is suitable for model validation[27]. The high spatial resolution allows the observation of the shear and curvature of E_r in the transport barrier, so that their role on ETBs formation can be analyzed separately. This discharge shows a long period of secular increase in the edge ion temperature gradient after a "soft" L-H transition having a longer time-scale (a few hundred milliseconds) in comparison with a conventional "hard" one having shorter time-scale (*e.g.* a few milliseconds or less) seen in many tokamaks. This is followed by a violent phase, where the edge plasma bifurcates between a strong-E_r and a weak-E_r state (occurred at the normalized electric field condition of $\frac{e\rho_\theta |E_r|}{T_i} \approx 1$[28], where the ρ_θ is the ion poloidal gyro-radius), until it finally settles to the conventional H-mode. The time period of $0 < \Delta t_{\text{L-H}} < 0.3$ s in Fig. 1(a) is considered to be quasi-stationary for turbulence evolution and is suitable in evaluating the influence of inhomogeneous E_r.

Looking at the slow L-H transition phase ($0 < \Delta t_{\text{L-H}} < 0.3$ s), we found that the $L_{T_i}^{-1}$ increases as the $\sqrt{Z}$ value becomes more positive, as shown in Fig. 1(a,b). The main contribution to the change of Z is from Z_2, and Z_1 remains small during the growth of the temperature gradient. An important caveat to this discussion is that there

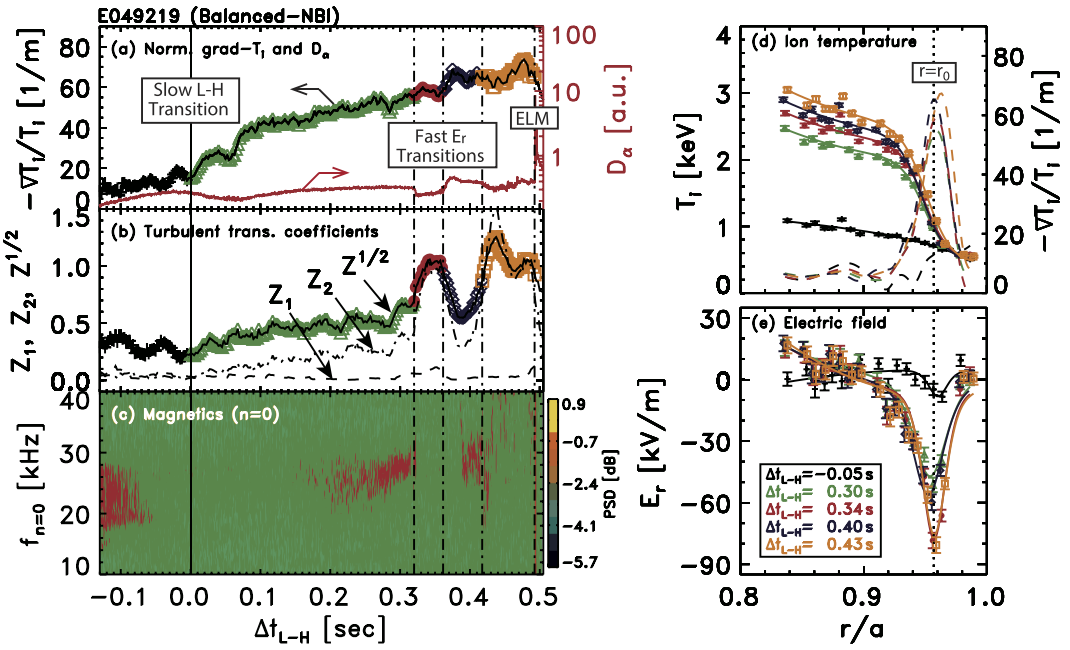

Figure 1. Temporal evolutions for (**a**) normalized ion temperature gradient ($L_{T_i}^{-1} \equiv -\nabla T_i/T_i$) and D_α emission, (**b**) $Z_1 \propto E_r' E_r'$, $Z_2 \propto -E_r^* E_r''$ and square root of $Z(\equiv Z_1 + Z_2)$ as defined in Eq. 2, and (**c**) Frequency and time resolved spectrogram for n = 0 component in the magnetic fluctuation detected by the sum of eight channel saddle loop arrays (toroidal). Radial profiles for (**d**) ion temperature and its inverse scale-length ($L_{T_i}^{-1} \equiv -\nabla T_i/T_i$), and (e) radial electric field are also shown. Vertical dotted line ($r \equiv r_0$) for (**d**) and (**e**) corresponds to the location at which the $L_{T_i}^{-1}$ has a local peak value. Temporal evolutions for $L_{T_i}^{-1}$, $Z^{1/2}$, Z_1, and Z_2 are evaluated at $r = r_0$.

is only a low correlation between Z_1 and $L_{T_i}^{-1}$ at which $L_{T_i}^{-1}$ has a peak value in the pedestal (defined by $r \equiv r_0$ as illustrated in Fig. 1d), while the $L_{T_i}^{-1}$ value at $r = r_0$ becomes large as the Z_2 value at $r = r_0$ increases. This shows the relative importance of nonzero second derivative effect ($\propto E_r E_r''$) with its sign dependence for the turbulent suppression rather than that of the first derivative effect ($\propto E_r' E_r'$), especially for the ETBs region around $r = r_0$ (the effect of E_r-shear/curvature on other remaining region in the pedestal, such as $r \leq r_0$, will be discussed later). It should be noted that the location at which the $L_{T_i}^{-1}$ has a local peak value (i.e. $r = r_0$) is closely related to that at which the E_r (and/or its curvature) has a local peak value as shown in Fig. 1(d,e), where the E_r-shear has almost zero value. Indeed, this fact is confirmed by a quantitative comparison for various pedestal structures obtained in JT-60U H-mode plasmas with different angular momentum injections (*e.g.* co- and counter-NBI plus perpendicular-NBI heating)[29].

It is interesting that a uniform toroidal MHD oscillation (i.e. $n = 0$) seems to be associated with the multi-stage E_r-transitions during ELM-free H-phase as shown in Fig. 1(c). Since the frequency dependence of this MHD mode ($f_{GAM} \approx C_s/2\pi R$) is likely to that of the predicted frequency for Geodesic Acoustic Mode (GAM) known as a high-frequency blanch of Zonal flow (ZF), this observation can also support the hypothesis of ZF (and/or E_r-curvature) suppression of turbulence even in the H-mode plasmas.

The quantitative comparison between the temperature gradient and inhomogeneity effect of electric field is illustrated in Fig. 2. In the slow L-H transition phase ($\Delta t_{L\text{-}H} = 0.0$–$0.32\,s$) there is a good correlation between the $\frac{L_{T_i}^{-1}(H-phase)}{L_{T_i}^{-1}(L-phase)}$ and $\sqrt{Z}$ at $r = r_0$. The enhancement of the gradient (by the factor of a few times) appears in the range of $\sqrt{Z} \sim 0.5$. The observed proportionality between increased gradient and $\sqrt{Z}$ is to hold approximately $\frac{L_{T_i}^{-1}(H-phase)}{L_{T_i}^{-1}(L-phase)} \sim 10\sqrt{Z}$. It is in the range of expectation with the assumption of $k\rho_i \sim 0.1$–0.3.

The relationship between $\frac{L_{T_i}^{-1}(H-phase)}{L_{T_i}^{-1}(L-phase)}$ and the parameter Z shows a more complex (*i.e.* non-linear) behaviour after $\Delta t_{L\text{-}H} = 0.32\,s$, where $\sqrt{Z} \geq 0.5$. During the phase $\Delta t_{L\text{-}H} = 0.32$–$0.36\,s$, a fast (within milliseconds) and strong drop in D_α emission can be seen (Fig. 1a), while the increase in the $\frac{L_{T_i}^{-1}(H-phase)}{L_{T_i}^{-1}(L-phase)}$ seems to be lower (up to about 10% or less). This suggests that there are additional mechanisms in the final stage of the H-mode transition in addition to the mechanism included in Eqs 1 and 2. At $\Delta t_{L\text{-}H} = 0.36\,s$, the D_α emission increases rapidly, and dramatic changes in the edge E_r structure from strong-E_r to weak-E_r are visible. These changes are similar to those at $\Delta t_{L\text{-}H} = 0.42\,s$, but the changes are in opposite direction. However, this does not seem to be the same as the H-L backward transition commonly associated with the L-mode but, rather, this phase ($\Delta t_{L\text{-}H} = 0.36$–$0.42\,s$) seems to

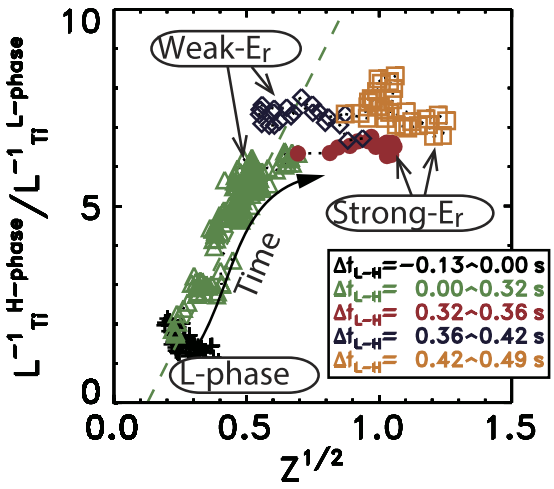

Figure 2. Relationship between the $\frac{L_{T_i}^{-1}(H-phase)}{L_{T_i}^{-1}(L-phase)}$ and $\sqrt{Z}$ ($\propto\sqrt{E_r'E_r' - E_r^*E_r''}$ as defined in Eq. 2) at which the $L_{T_i}^{-1}$ (and/or Er) has a local peak value for discharge E049219 (balanced-NBI). The line (dashed) $Y = -1.7 + 13.4\,X$ is drawn, where Y is $\frac{L_{T_i}^{-1}(H-phase)}{L_{T_i}^{-1}(L-phase)}$ and X is $\sqrt{Z}$, in which we use X and Y data for the slow L-H transition phase ($\Delta t_{L\text{-}H} = 0.0 - 0.32$ sec).

be similar to the phase $\Delta t_{L\text{-}H} = 0.0$–$0.32\,s$. After $\Delta t_{L\text{-}H} = 0.42\,s$, the plasma changes again, with characteristics similar to the phase $\Delta t_{L\text{-}H} = 0.32$–$0.36\,s$. This phase continues until the first ELM onset at $\Delta t_{L\text{-}H} = 0.49\,s$.

The question why the dependence of $\frac{L_{T_i}^{-1}(H-phase)}{L_{T_i}^{-1}(L-phase)}$ on $\sqrt{Z}$ at $r = r_0$ is likely to be non-linear, especially for the later ELM-free H-phase (during $\Delta t_{L\text{-}H} = 0.32$–$0.36\,s$ and $\Delta t_{L\text{-}H} = 0.42$–$0.49\,s$), requires further studies: Let us explain a hypothesis to understand this stimulating observation. Before the jump of electric field occurs, the suppression of turbulence is strong enough so that the ion thermal transport is reduced to the level of the neoclassical transport. The abrupt bifurcations in the edge E_r to larger values (say, $Z \sim 1$), suppress the turbulence as was shown in[27], so as to induce the jumps in D_α emission. However, the ion thermal transport is less sensitive, owing to the remaining neoclassical thermal transport for ions. Indeed, we confirm that the dependence of $\frac{L_{T_i}^{-1}(H-phase)}{L_{T_i}^{-1}(L-phase)}$ on $\sqrt{Z}$ at $r = r_0$ seems to be almost linear for the slow L-H transition phase having weak E_r ($\Delta t_{L\text{-}H} = 0.0$–$0.32\,s$), including another phase having weak E_r ($\Delta t_{L\text{-}H} = 0.36$–$0.42\,s$), as expected from Eq. 3.

Experimental results (II): Spatial dynamics in ELMing phase. Experimental data presented in Fig. 3 exhibit the highest quality data that is also suitable for model validation in a different perspective, especially for the relationship between pedestal width and thickness of the inhomogeneous edge E_r layer. These data are determined from multiple and reproducible Edge Localized Modes (ELMs) cycles for co- and counter-NBI discharges, mapping them onto a single-time basis, as defined by the time of the measurement relative to the ELMs for improved statistics to assess the temporal behavior (in particular inter-ELM phase) of the measurements[29].

As shown in Fig. 3(c), the pedestal width (evaluated at the cross-point of the $L_{T_i}^{-1}$ profiles between L- and H-mode phases) seems to be expanded up to $R\text{-}R_{SEP} \geq -0.08$ m for co-NBI case, while it becomes narrower up to $R\text{-}R_{SEP} \geq -0.06$ m for counter-NBI case. Looking at Fig. 3(e,f), we found that non-zero Z_1 layer (i.e. impact of the E_r-shear on turbulence suppression is effective) seems to be restricted in a range of $R\text{-}R_{SEP} \geq -0.07$ m (co-NBI) and -0.05 m (counter-NBI), respectively, indicating about 1 cm narrower than that of the pedestal width. Furthermore, there is Z_2 layer of the negative value (contributing turbulence enhancement) around $R\text{-}R_{SEP} \approx -0.04$ m in the counter-NBI case.

It should be noted that we found a strong correlation between the location at which the $L_{T_i}^{-1}$ and E_r (and/or its curvature) had a local peak values for both co- and counter-NBI cases as shown in solid line on Fig. 3(g). On the other hand, the location at which the E_r-shear had a local peak value shift inwards from the radius where the $L_{T_i}^{-1}$ had a local peak value. The difference of the positions of the peak of E_r' and $L_{T_i}^{-1}$ is confident, beyond the error bar, although we could see a linear correlation (i.e. direct proportion excepting its proportionality coefficient) between them. This conclusion holds for both co- and counter-NBI cases as shown in dotted line on Fig. 3(g). The most important point on this discussion is that we could confirm the conclusion in the ELM-free phase [i.e. the relative importance of nonzero second derivative effect ($\propto E_r E_r''$) for the turbulent suppression rather than that of the first derivative effect ($\propto E_r' E_r'$)], being described in Fig. 1d,e] even in the ELMing phase much more accurately.

As a result, we found the Z-profile had almost non-zero value in the pedestal region (at least for its full width at half maximum of $\frac{L_{T_i}^{-1}(H-phase)}{L_{T_i}^{-1}(L-phase)}$ value) for both co- and counter-NBI cases as shown in Fig. 4(a,b). Furthermore, we confirmed that the dependence of the $\frac{L_{T_i}^{-1}(H-phase)}{L_{T_i}^{-1}(L-phase)}$ value on $\sqrt{Z}$ exhibited a similar trend for both co- and

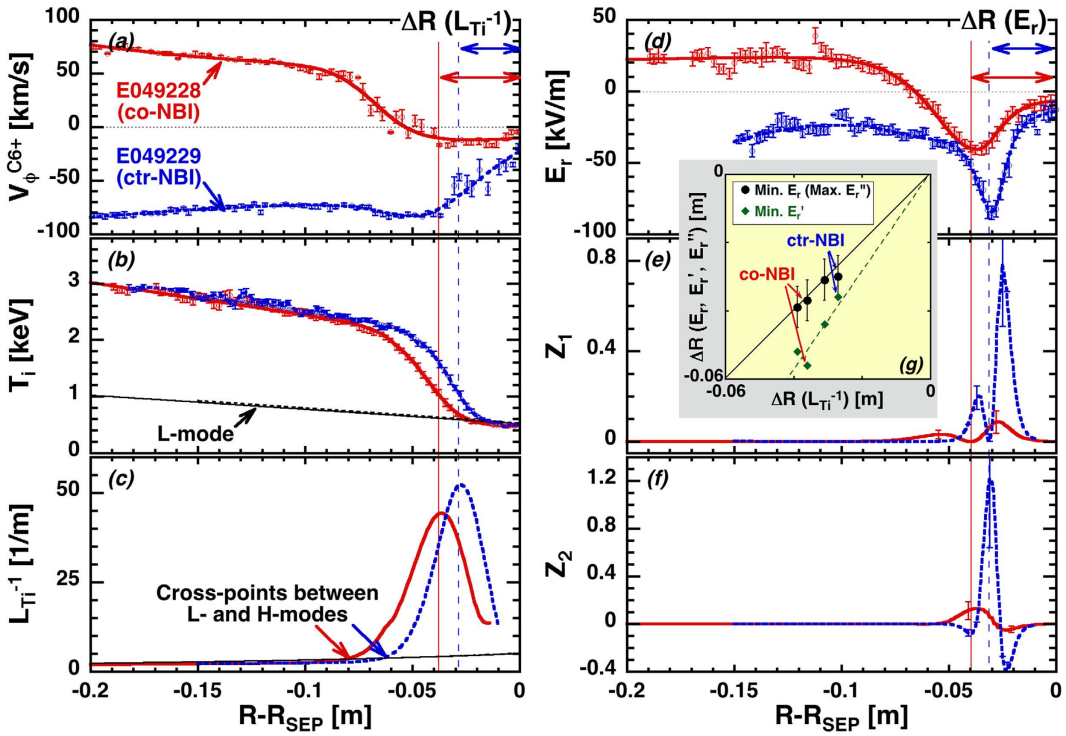

Figure 3. Radial profiles for (**a**) toroidal rotation for fully-stripped carbon impurity ions, (**b**) ion temperature, T_i, (**c**) inverse ion temperature scale-length ($L_{T_i}^{-1} \equiv -\nabla T_i/T_i$), (d) radial electric field, E_r, (**e**) $Z_1 \propto E_r' E_r'$ and (**f**) $Z_2 \propto -E_r^* E_r''$ as defined in Eq. 2 in the discharges E049228 (co-NBI) and E049229 (ctr-NBI). Vertical lines (solid line: co-NBI, dashed line: ctr-NBI) are drawn for the locations at which the $L_{T_i}^{-1}$ and E_r have a local peak values [defined as $\Delta R(L_{T_i}^{-1})$ and $\Delta R(E_r)$, respectively], exhibiting a strong correlation between $\Delta R(L_{T_i}^{-1})$ and $\Delta R(E_r)$ for various pedestal structures obtained in JT-60U H-mode plasmas with different angular momentum injections as summarized in (**g**).

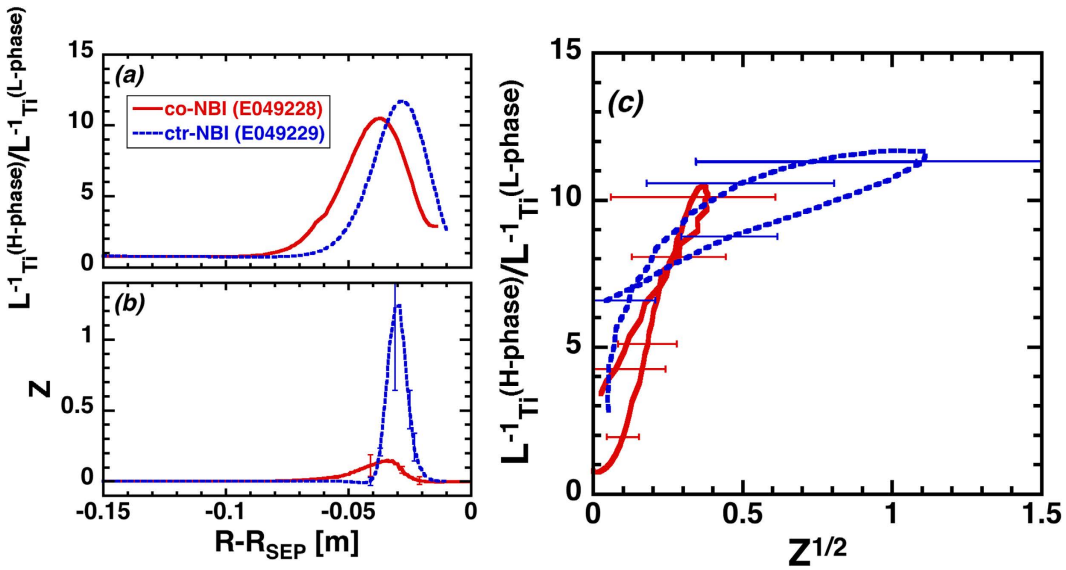

Figure 4. Radial profiles for (**a**) ratio of the inverse ion temperature scale-length ($L_{T_i}^{-1} \equiv -\nabla T_i/T_i$) in H- to L-phases, $\frac{L_{T_i}^{-1}(H-phase)}{L_{T_i}^{-1}(L-phase)}$, (**b**) effect of an inhomogeneous radial electric field on the turbulence suppression predicted by the E_r-bifurcation model, $Z \propto (E_r' E_r' - E_{r_i}^* E_r'')$ as defined in Eq. 2 in the discharges E049228 (co-NBI) and E049229 (counter-NBI). Relationship between $\frac{L_{T_i}^{-1}(H-phase)}{L_{T_i}^{-1}(L-phase)}$ versus square root of Z is also shown in (**c**).

counter-NBI cases as illustrated in Fig. 4(c). It should be noted that the relationship between those factors obtained in the ELM-free phase at a fixed location (i.e. $r = r_0$ defined for discharge E049219) shows a similar nature to that obtained even in the ELMing phase (at the time of ELM-onset) for various locations (discharges E049228 and E049229).

This result is not self-evident, since the Z value in the latter case (i.e. spatial structure in the ELMing phase) contains both E_r-shear and E_r-curvature effects, while the E_r-curvature effect is dominant contributor for Z value in the former case (i.e. temporal trajectory in the ELM-free phase).

It is also noted that the improved energy confinement region (*e.g.* $\frac{L_{T_i}^{-1}(H-phase)}{L_{T_i}^{-1}(L-phase)} > 1$) is observed even in the region near the pedestal top, where Z value is small. The smooth connection phenomena between L-mode region (*e.g.* around the pedestal-top) and H-mode pedestal (*e.g.* well inside the pedestal-top) results in an up-shift of the curve in Fig. 4(c), in comparison with that seen in Fig. 2.

Discussion and Summary. In summary, we revisited the studies of paradigm of shear suppression of turbulence as the mechanism for the ETBs formation with an improved diagnostic for the edge radial electric field from the high resolution measurement on JT-60U tokamak, examining the effects of both shear and curvature, comparing with E_r-bifurcation model. Focusing on the relationship between the normalized ion temperature gradient and non-uniform radial electric field structures, we found that E_r-curvature effects are essential, (not only the E_r-shear) in forming the ETBs. Recalling that the non-uniform E_r effect presented in this letter should have 2nd order effect of $\boldsymbol{O}(E_r^2)$, the Z profile is localized strongly around the location, at which the $L_{T_i}^{-1}$ has a local peak value in the pedestal, and hence inhomogeneous electric field seen in the H-mode pedestal makes it possible to have an impact on the turbulence suppression even at the lower edge of the pedestal structure.

Indeed, this effect may be able to exude toward the pedestal top (and/or bottom) due to its 2nd order effect, leading a new prediction of the pedestal width scaling (and/or providing an possible physics understanding for its scaling using non-dimensional parameters in many tokamas). It should be noted that the thickness in the $\boldsymbol{E} \times \boldsymbol{B}$ shear layer was roughly scaled by a few times of the ρ_{θ_i} in the previous publication based on a poor spatial resolution[34]. It is also suggested that there is additional mechanism to regulate the temperature gradient in the fully developed H-mode plasmas[35].

Methods

JT-60U. The JT-60U tokamak is a single null divertor tokamak device having the plasma major radius, $R_p = 3$–3.5 m, the plasma minor radius, $a_p = 0.6$–1.1 m and the maximum toroidal magnetic field, $B_T \leq 4$ T at $R = 3.32$ m. We performed the NBI heating experiments by comparing the external momentum input directions between co-, balanced- and counter-NBI cases under a matched plasma shape condition. The plasma current, I_p, was 1.6 MA, and the toroidal magnetic field, B_T, was 3.9 T. The corresponding safety factor at the 95% flux surfaces, q_{95}, was thus 4.2. The elongation, κ, and triangularity, δ, were 1.47 and 0.36, respectively, and the total plasma volume was 57 m^3.

Charge eXchange Recombination Spectroscopy (CXRS). In the study of the JT-60U tokamak for the fiscal year (FY) 2007–2008 experimental campaign, we measured the radial profiles for the density, temperature, and poloidal/toroidal plasma flows of fully stripped carbon impurity ions by means of the Charge eXchange Recombination Spectroscopy (CXRS) diagnostic method with fast time resolution (up to 400 Hz) at 59 spatial points (23 toroidal and 36 poloidal viewing chords). With regard for determining the E_r structure at the pedestal region, we measured the pressure gradient, and plasma velocity perpendicular to the magnetic field, and the E_r was evaluated by the radial force balance equation.

References

1. Wagner, F. *et al.* Regime of Improved Confinement and High Beta in Neutral-Beam-Heated Divertor Discharges of the ASDEX Tokamak. *Phys. Rev. Lett.* **49,** 1408 (1982).
2. ITER Physics Basis, *Nucl. Fusion* **39,** 2137 (1999).
3. Itoh, S.-I. & Itoh, K. Model of *L* to *H*-Mode Transition in Tokamak. *Phys. Rev. Lett.* **60,** 2276 (1988).
4. Shaing, K. C. & Crume, E. C. Jr. Bifurcation Theory of Poloidal Rotation in Tokamaks: A Model for the *L*-*H* Transition. *Phys. Rev. Lett.* **63,** 2369 (1989).
5. Biglari, H., Diamond, P. H. & Terry, P. W. Influence of sheared poloidal rotation on edge turbulence. *Phys. Fluids* **B2,** 1 (1990).
6. Itoh, K. & Itoh, S.-I. The role of the electric field in confinement. *Plasma Phys. Control. Fusion* **38,** 1–49 (1996).
7. Groebner, R. J., Burrell, K. H. & Seraydarian, R. P. Role of edge electric field and poloidal rotation in the L-H transition. *Phys. Rev. Lett.* **64,** 3015 (1990).
8. Ida, K. *et al.* Edge electric-field profiles of H-mode plasmas in the JFT-2M tokamak. *Phys. Rev. Lett.* **65,** 1364 (1990).
9. Burrell, K. H. *et al.* Physics of the L-mode to H-mode transition in tokamaks. *Plasma Phys. Control. Fusion* **34,** 1859 (1992).
10. Burrell, K. H. Effects of E×B velocity shear and magnetic shear on turbulence and transport in magnetic confinement devices. *Phys. Plasmas* **4,** 1499 (1997).
11. Ida, K. Experimental studies of the physical mechanism determining the radial electric field and its radial structure in a toroidal plasma. *Plasma Phys. Control. Fusion* **40,** 1429 (1998).
12. Shaing, K. C., Crume, E. J. & Houlberg, W. A. Bifurcation of poloidal rotation and suppression of turbulent fluctuations. A model for the L-H transition in tokamaks *Phys. Fluids B* **2,** 1492 (1990).
13. Zhang, Y. Z. & Mahajan, S. M. Edge turbulence scaling with shear flow. *Phys. Fluids B* **4,** 1385 (1992).
14. Waltz, R. E., Kerbel, G. O. & Milovich, J. Toroidal gyro-Landau fluid model turbulence simulations in a nonlinear ballooning mode representation with radial modes. *Phys. Plasmas* **1,** 2229 (1994).
15. Terry, P. W. Suppression of turbulence and transport by sheared flow. *Rev. Modern Physics* **72,** 109 (2000).
16. Staebler, G. M. & Dominguez, R. R. Electric field effects on ion temperature gradient modes in a sheared slab. *Nucl. Fusion* **31,** 1891 (1991).

17. Diamond, P. H. *et al.* Self-Regulated Shear Flow Turbulence in Confined Plasmas: Basic Concepts and Potential Applications to the L-H Transition. *Proceedings of the Fourteenth International Conference on Plasma Physics and Controlled Nuclear Fusion Research 1993* (Wurzburg, Germany, 30 September - 7 October, 1992), IAEA, Vol. 2, 1993 (pp. 97–113).
18. Dominguez, R. R. & Staebler, G. M. Anomalous momentum transport from drift wave turbulence. *Phys. Fluids B* **5,** 3876 (1993).
19. Itoh, S.-I., Itoh, K., Fukuyama, A. & Yagi, M. Theory of Anomalous Transport in H-Mode Plasmas. *Phys. Rev. Lett.* **72,** 1200 (1994).
20. Moyer, R. A. *et al.* Beyond paradigm: Turbulence, transport, and the origin of the radial electric field in low to high confinement mode transitions in the DIII-D tokamak. *Phys. Plasmas* **2,** 2397 (1995).
21. Taylor, J. B., Connor, J. W. & Helander, P. On transport barriers and low–high mode transitions. *Phys. Plasmas* **5,** 3065 (1998).
22. Diamond, P. H., Itoh, S.-I., Itoh, K. & Hahm, T. S. Zonal flows in plasma—a review. *Plasma Phys. Control. Fusion* **47,** R35 (2005).
23. Ida, K. *et al.* Transition between Internal Transport Barriers with Different Temperature-Profile Curvatures in JT-60U Tokamak Plasmas. *Phys. Rev. Lett.* **101,** 055003 (2008).
24. Kaw, P., Singh, R. & Diamond, P. H. Coherent nonlinear structures of drift wave turbulence modulated by zonal flows. *Plasma Phys. Control. Fusion* **44,** 51 (2002).
25. Fujisawa, A. *et al.* Causal Relationship between Zonal Flow and Turbulence in a Toroidal Plasma. *J. Phys. Soc. Jpn.* **76,** 033501 (2007).
26. Tokuzawa, T. *et al.* Observation of multi-scale turbulence and non-local transport in LHD plasmas. *Phys. Plasmas* **21,** 055904 (2014).
27. Kamiya, K. *et al.* Observation of a Complex Multistage Transition in the JT-60U H-mode Edge. *Phys. Rev. Lett.* **105,** 045004 (2010).
28. Kamiya, K. *et al.* Edge Radial Electric Field Formation after the L-H Transition on JT-60U. *Contrib. Plasma Phys.* **54,** 591 (2014).
29. Kamiya, K. *et al.* Boundary condition for toroidal plasma flow imposed at the separatrix in high confinement JT-60U plasmas with edge localized modes and the physics process in pedestal structure formation. *Phys. Plasmas* **21,** 122517 (2014).
30. Doyle, E. J. *et al.* Chapter 2: Plasma confinement and transport. *Nucl. Fusion* **47,** S18 (2007).
31. Itoh, K., Itoh, S.-I., Kamiya, K. & Kasuya, N. On the spatial structure of solitary radial electric field at the plasma edge in toroidal confinement devices. *Plasma Phys. Control. Fusion* **57,** 075008 (2015).
32. Itoh, K. *et al.* On the origin of steep radial electric field in the transport barrier at plasma edge. *Contrib. Plasma Physics*, doi: 10.1002/ctpp.201610042 (2016).
33. Connor, J. W. *et al.* An assessment of theoretical models based on observations in the JET tokamak: I. Ion heat transport due to ∇Ti instabilities. *Plasma Phys. Control. Fusion* **35,** 319 (1993).
34. Ida, K. *et al.* Thickness of ExB Velocity Shear at the Plasma Edge in the JFT-2M H-mode. *Plasma Phys. Control. Fusion* **36,** A279 (1994).
35. Itoh, K., Itoh, S.-I., Kamiya, K. & Kobayashi, T. On Width and Height of Pedestal in the H-mode. *Nucl. Fusion* **56,** in press (2016).

Acknowledgements

The authors deeply appreciate the continued research and operational efforts of the entire JT-60 team. Discussions with Prof. K. Ida, Dr. T. Kobayashi, Prof. P. H. Diamond, Prof. U. Stroth and Prof. J. Q. Dong are also acknowledged. Authors acknowledge the partial support by Grant-in-Aid for Scientific Research (15K06657, 15H02155, 16H02442) and collaboration programmes between QST and universities and of the RIAM of Kyushu University, and by Asada Science Foundation.

Author Contributions

K.K. analyzed the data. K.I. and S.-I.I. provided the theoretical models. K.K., K.I. and S.-I.I. discussed the model validation. K.K. and K.I. wrote the main manuscript text and all authors reviewed the manuscript.

Additional Information

Competing financial interests: The authors declare no competing financial interests.

How to cite this article: Kamiya, K. *et al.* Experimental validation of non-uniformity effect of the radial electric field on the edge transport barrier formation in JT-60U H-mode plasmas. *Sci. Rep.* **6**, 30585; doi: 10.1038/srep30585 (2016).